

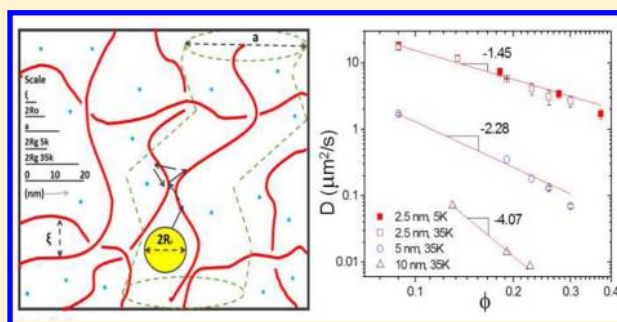
## Diffusion of Nanoparticles in Semidilute Polymer Solutions: Effect of Different Length Scales

Indermeet Kohli and Ashis Mukhopadhyay\*

Department of Physics and Astronomy, Wayne State University, Detroit, Michigan 48201, United States

## Supporting Information

**ABSTRACT:** We used gold nanoparticles (NPs) to investigate the length-scale-dependent dynamics in semidilute poly(ethylene glycol) (PEG)–water solutions. Fluctuation correlation spectroscopy was used to measure the diffusion coefficients ( $D$ ) of the NPs as a function of their radius ( $R_0$ ), PEG volume fraction ( $\phi$ ), and molecular weight ( $M_w$ ). Our results indicate that the radius of gyration,  $R_g$ , of polymer chain is the crossover length scale for the NPs experiencing nanoviscosity or macroviscosity. The reduced diffusivity can be plotted on a single master curve as  $D_0/D = \exp(\alpha(R_0/\xi)^\delta)$  for  $R_g > R_0$  and as  $D_0/D = \exp(\alpha(R_g/\xi)^\delta)$  for  $R_g \leq R_0$ , where  $D_0$  is the diffusion coefficient in neat solvent,  $\xi$  is the correlation length,  $\alpha = 1.63$ , and  $\delta = 0.89$ . In size regime,  $\xi < R_0 < a(\phi)$ , where  $a(\phi)$  is the tube diameter for entangled polymer liquid, we found  $D \sim \phi^{-1.45}$  and independent of  $M_w$ . For  $R_0 > a(\phi)$ ,  $D \sim \phi^{-4}$  was obtained.



## INTRODUCTION

Understanding the transport properties of nanoparticles (NPs) in solutions of macromolecules is important for several interdisciplinary fields of studies as well as relevant for many technological applications. For example, in colloidal physics, the diffusion and sedimentation of particles play a vital role for the dispersion stability, analytical separation, and chromatography.<sup>1</sup> In biophysics, there is growing interest to understand how biopolymers such as proteins move through crowded cytoplasmic environments.<sup>2</sup> The dynamics in this situation can affect cellular functions, such as kinetics of enzymatic reactions, the formation of DNA or protein complexes, and self-assembly of various supramolecular structures, like fibrillar aggregates.<sup>3</sup> In the areas of soft matter physics and nanotechnology, these studies are important for proper interpretation of microrheology experiments<sup>4</sup> and development of novel composite systems that contained nanosized inclusions.<sup>5</sup>

For many of these reasons, diffusion of NPs in polymer solutions has received a lot of attention theoretically<sup>6–11</sup> as well as experimentally.<sup>9,11–16</sup> In simple liquids, the translational diffusion coefficient ( $D$ ) of isolated spherical particles is given by the well-known Stokes–Einstein (SE) relation,  $D = k_B T / 6\pi\eta_0 R_0$ , where  $k_B$  is the Boltzmann constant,  $T$  is the absolute temperature, and  $\eta_0$  is the solvent viscosity. It is assumed in this relation that the radius of the particle ( $R_0$ ) is much greater than solvent molecules.<sup>12</sup> But in a ternary mixture containing polymer, solvent, and the particle, there are several length scales involved and application of SE relation becomes complicated in certain regimes. In semidilute solutions, where the polymer concentration is above the overlap volume fraction ( $\phi^*$ ), the matrix forms a transient network of overlapping chains

characterized by an average mesh size called the correlation length ( $\xi$ ).<sup>17,18</sup> It is a decreasing function of polymer volume fraction ( $\phi$ ),  $\xi \sim \phi^{-0.76}$ , for uncharged polymers in good solvent and is independent of the polymer molecular weight ( $M_w$ ). The correlation length introduces a new length scale in addition to particle radius and the radius of gyration of the polymer chain ( $R_g$ ). Theoretical approaches by de Gennes and co-workers have identified three regimes depending on the relative size ratio,  $R_0/\xi$ .<sup>17,19</sup> If  $R_0/\xi \ll 1$ , the particles can slip easily through the mesh, and they detect only the neat solvent viscosity ( $\eta_0$ ). In the opposite limit, the diffusion is governed by the macroscopic viscosity ( $\eta_m$ ) of the solution, which is commonly measured in a rheometer. In the transition regime,  $R_0/\xi \sim 1$ , the local viscosity ( $\eta_\phi$ ) experienced by the particle depends upon the length scales at which it is probed, and generally  $\eta_0 < \eta_\phi < \eta_m$ . In this scenario,  $\xi$  can be considered as the “crossover length scale”, and  $\eta_\phi$  depends upon  $\phi$ , but independent of  $M_w$ . A scaling relation of the form  $D_0/D = \eta_\phi/\eta_0 \sim F(R_0/\xi)$  has been suggested, where  $D_0$  is the diffusion coefficient of the particle in the neat solvent.<sup>9</sup> Some theoretical models have suggested a functional form,  $F(R_0/\xi) \sim \exp(R_0/\xi)$ . But there are conflicting reports in the literature regarding the validity of these predictions.<sup>9,12,13,16,20–23</sup> A competing model of probe diffusion was developed by Phillies.<sup>6</sup> He argued that hydrodynamic interactions dominate over topological constraints on probe diffusion and proposed an equation of the form  $D/D_0 \sim \exp(-\beta\phi^\nu)$ .<sup>6,24,25</sup> Though regarded mostly as an

Received: June 18, 2012

Revised: July 18, 2012

Published: July 27, 2012

empirical equation, it fits a wide range of concentration from dilute to concentrate as well as probes and polymers with different architectures (linear, branched, globular, star-shaped, etc.).<sup>11</sup> Phillies noted that  $\beta$  depends upon  $M_w$  but is independent of  $R_0$ , and  $\nu$  depends upon solvent quality ranging from 0.5 to 1. Hydrodynamic screening theory by Cukier predicts a similar form,  $D/D_0 \sim \exp(-\kappa R_0/\xi)$ , which yields the exponent  $\nu = 0.76$ .<sup>7</sup> Recent theoretical approaches have considered the effect of depletion layer for neutral polymer–probe interaction.<sup>26</sup> Such a layer has a thickness of the order of  $\xi$ , where the segmental density of the chain increases from zero to the bulk value.<sup>26</sup> Assuming that the local viscosity is a function of monomer concentration, it gradually increases from the solvent viscosity ( $\eta_0$ ) close to the probe surface to macroviscosity ( $\eta_m$ ) in the bulk.<sup>27</sup> The analysis also showed a stretched exponential function for  $F(R_0/\xi)$  in semidilute solution.<sup>8</sup> None of these theories consider explicitly the dynamical characteristics of the polymer matrix. A recent scaling theory by Cai et al. have considered the effect of chain relaxation on the mobility of particles.<sup>28</sup> They have derived the power law dependencies of polymer concentration and particle size on diffusion coefficient. In parallel to the theoretical approaches, there have been molecular dynamics simulations as well, which found that the crossover length scale between nano- and macroviscosity is not  $\xi$ , but  $R_g$ .<sup>10,29,30</sup> For unentangled melts, in regime  $R_0 < R_g$ , local viscosity ( $\eta_\phi$ ) is dominated by monomer units rubbing the nanoparticle surface, making it proportional to the particle area ( $R_0^2$ ), which yields  $D \propto 1/R_0^3$  and independent of chain length. In the large particle limit, hydrodynamic contribution dominates giving  $D \propto 1/R_0$ , and its numeric value is given by SE relation of diffusion coefficient ( $D_{SE}$ ).<sup>29,30</sup>

Experimentally, dynamic light scattering (DLS),<sup>15,21,27,31</sup> fluctuation correlation spectroscopy (FCS),<sup>13,14,23,32</sup> fluorescence recovery after photobleaching (FRAP),<sup>12</sup> and sedimentation<sup>9,15,20,21</sup> are most popular in this area of research. A recent review of experiments could be found in ref 14, and some of the earlier works were well summarized in ref 22. We will briefly mention only few results, which will help readers to put our work in perspective. DLS experiments by the Lodge group<sup>22</sup> have found that for polystyrene spheres ( $R_0 \approx 200$  nm) in solutions of poly(vinyl methyl ether) with  $R_g \approx 54$  nm the ratio  $D/D_{SE}$  increases with the polymer concentration and reaches the maximum value of  $\approx 3$  near  $\phi^*$ . But sufficiently above the entanglement concentration,  $\phi_e$  ( $\approx 3\phi^*$ ), the SE behavior was recovered. DLS experiments measured the diffusion at a short length scale compared to  $R_0$ , which is perturbed significantly by the depletion layer and may not record the average bulk behavior.<sup>15,21,22,26,27</sup> Sedimentation and FCS experiments, in contrast, probe the long-time and large-scale motion of the particles.<sup>9,15</sup> Sedimentation experiments have found that the particles experience the single-chain viscosity rather than the solvent viscosity when  $R_0 < \xi$ .<sup>21</sup> In the intermediate region,  $D_0/D$  does not have the simple scaling form  $F(R_0/\xi)$  and depends upon  $M_w$ .<sup>20</sup> As the polymer concentration is increased and the limit,  $R_0 \gg \xi$  is reached, the particle feels the macroscopic viscosity as suggested by de Gennes theory. In these experiments, particle size ( $R_0 = 4$ – $5$  nm) was smaller than the radius of gyration ( $R_g = 8$  nm) of the chain. But a significant number of other experiments have reported deviation from SE equation when  $R_0 < R_g$ . The Hoyst group has performed FCS experiments with poly(ethylene glycol) (PEG) in water using probes as molecules with different

sizes, such as fluorescent dyes, proteins, and silica spheres.<sup>14</sup> They concluded that for  $2R_0 < R_g$  the measured nanoviscosity was orders of magnitude smaller than macroviscosity; however, macroviscosity governs the probe dynamics if  $2R_0 > R_g$ . In the crossover regime ( $2R_0 \sim R_g$ ), they observed a scale-dependent diffusion, which they explained in terms of nonuniform viscosity within the depletion layer.<sup>27</sup> The SE relation for larger probes in poly(vinyl alcohol) (PVA) solution was also verified in another FCS experiments by Michelman-Ribeiro et al.<sup>23</sup>

All the conflicting results regarding the crossover length scale and the roles of various parameters, such as mesh size, matrix dynamics, effect of entanglement, polymer–probe interaction, etc., demand further investigations. But it remains a challenge to study nanoparticle dynamics in a systematic manner, more specifically in the length regime  $\xi \leq R_0 < R_g$ . One of the reasons is the paucity of suitable probes in the size range of 5–20 nm.<sup>12</sup> For smallest sized probes ( $R_0 \sim 1$ – $2$  nm), different dyes (e.g., rhodamine, alexa), intermediate sizes ( $R_0 \sim 3$ – $5$  nm), fluorescently labeled molecules (e.g., dextran, lysozyme, bovine serum albumin), and larger sizes ( $R_0 \sim 5$ – $100$  nm) quantum dots, silica, and polystyrene spheres were used in previous experiments.<sup>12,14,23,25,27,31</sup> For the intermediate size, which is the focus of this study, the probes used so far were flexible and porous.<sup>12</sup> They can change their size depending upon the solvent condition or as the polymer concentration is varied. The solvent needs to be the poor solvent for the probe molecules, so that they adopt a compact globular structure. The use of different molecules can change the specific probe–polymer chemistry. As a result, the polymer density distribution near the particle surface may be altered and the properties of the depletion layer can be modified.<sup>4,21,26</sup> This can alter the viscous drag experienced by the particle and change the particles' diffusivity. There is evidence in computer simulation that diffusion coefficient could decrease with increasing interaction strength.<sup>30</sup>

In contrast to experiments by other groups, we have used rigid and impenetrable probes (gold spheres) with radius between 2.5 and 10 nm. The solvent (water) is a good solvent for the polymer at the room temperature, and the probe particles can also be readily dispersed into it. The use of the same probe but with different sizes eliminates the possibility of specific probe–polymer interaction that could change diffusion. Another distinguishing aspect of this research is the use of fluctuation correlation spectroscopy (FCS), which has the advantage of using extremely low particle concentrations ( $\sim$ few nM). This is about 4–5 orders of magnitude smaller compared to other methods such as DLS or FRAP. The average particle–particle separation is much higher, so that the mutual interactions between the particles can be neglected and only true self-diffusion was measured. The low concentration of particles also reduces the possibility of polymer-induced probe aggregation from depletion interaction. Because of the specificity of this technique, scattering from the matrix polymer does not significantly complicate the experiment or its interpretation. This is an issue in DLS experiments, where for smaller particles ( $R_0 < R_g$ ) and low concentration of particles, the autocorrelation function could be dominated by the dynamics of the polymer network.

In this paper we have used FCS to understand the nanoparticle dynamics in semidilute poly(ethylene glycol) (PEG) water solutions. The use of very small sized spherical probes well within the range  $\xi \leq R_0 < R_g$  made this study

unique. Our results will be important to test theories of polymer dynamics and understand the relationship between micro- and macroscopic viscosities of complex fluid systems. They will also have implications in other fields, where there is complex coupling between two or more characteristic length scales that govern their dynamics.

## MATERIALS AND METHODS

PEG samples of two different molecular weights 5 kg/mol ( $M_w/M_n = 1.08$ ) and 35 kg/mol ( $M_w/M_n = 1.15$ ) were purchased from Polymer Sources, Inc. Gold nanoparticles (Au NPs) of radius 2.5, 5, and 10 nm were purchased commercially from Corpuscular, Inc. Au NPs were particularly useful for our experiments as they do not photobleach like fluorescent dyes or blink like semiconductor quantum dots and their size can be tuned as desired. The scattering signal from small NPs is typically very low, but they have high luminescence efficiency upon multiphoton excitation.<sup>32</sup> The polydispersity of these nanoparticles is about 10% as was verified by transmission electron microscopy (TEM) experiments (Figure S1). The choice of the polymer molecular weights and particle sizes allow us to investigate the size regime that we are interested and also the transition process for the particles experiencing the nanoviscosity to macroviscosity. Many different concentrations of PEG ( $\phi = 0-0.37$ ) in water–Au NPs mixture as solvent were prepared using a digital balance with resolution of 1 mg. PEG has the advantage over other polymers such as polystyrene, which needs to be dissolved in organic solvents. These sometimes give a lot of background fluorescence and thus reduces signal-to-noise ratio. Control experiments indicated no strong interactions (e.g., ionic, covalent, etc.) between gold particle and PEG are present, which would have led to adsorption of polymers onto surfaces.

A Zeiss inverted microscope served as the experimental platform. Near-infrared light from an 800 nm, 80 MHz, femtosecond Ti:sapphire laser (Mai Tai, Spectra Physics) was focused on the sample through a high numerical aperture (NA = 1.25, 100 $\times$ ) objective. Emitted light was collected through the same objective and detected by two single photon counting modules (Hamamatsu). An integrated data acquisition system (ISS, IL) was used to record and analyze the output. As NPs diffuse in and out of the laser focus, the number of these particles fluctuates. This fluctuation ( $F$ ) is quantitatively studied through the autocorrelation function (ACF)  $G(\tau)$  given by

$$G(\tau) = \frac{\langle \delta F(t) \delta F(t + \tau) \rangle}{\langle F(t) \rangle^2}$$

If the cause of the fluctuation is Brownian diffusion, the diffusion coefficient ( $D$ ) can be calculated from the ACF by using

$$G(\tau) = \frac{G(0)}{1 + \left( \frac{8D\tau}{\omega_0^2} \right) \sqrt{1 + \left( \frac{8D\tau}{z_0^2} \right)}}$$

In the preceding equation,  $G(0)$  is the magnitude of ACF at short time which is inversely proportional to the number of particles within the laser focus,  $\omega_0$  is the half-width, and  $z_0$  is the half-height of the laser focus. We determined by a calibration experiment that  $\omega_0 \approx 0.25 \mu\text{m}$  and  $z_0 \approx 1 \mu\text{m}$ .

## RESULTS AND DISCUSSION

Before presenting the results, calculations of the important length scales of the system would be useful. The radius of gyration,  $R_g$ , of the PEG in water as a function of  $M_w$  is given by  $R_g = 0.02M_w^{0.58}$  (nm),<sup>33</sup> which corresponds to  $R_g = 2.8$  and 8.6 nm for 5K and 35K PEG. Since  $R_0$  ranges from 2.5 to 10 nm,  $R_0/R_g$  was varied from 0.9 to 4 for 5K and 0.3 to 1.2 for 35K PEG samples. The overlap volume fraction,  $\phi^*$ , which marks the onset of semidilute regime was determined by using the relation  $\phi^* = 3M_w/(4\pi\rho N_A R_g^3)$ , where  $\rho$  is the polymer density

and  $N_A$  is Avogadro's number.<sup>17</sup> We estimated that  $\phi^* = 0.08$  for PEG 5K and  $\phi^* = 0.02$  for PEG 35K. Our measurements were carried out in the range of  $\phi = 0.09-0.37$ , all of which were in the semidilute regime. The correlation length ( $\xi$ ) as a function of polymer concentration was calculated by using the relationship  $\xi \approx R_g(\phi/\phi^*)^{-0.76}$ . It indicates that  $\phi^*$  depends upon  $M_w$ , but  $\xi$  is nearly independent of it.  $\xi$  ranged from 0.95 to 2.6 nm. In all measurements  $R_0 \geq \xi$ , and the ratio  $R_0/\xi$  varied from  $\approx 1$  to 11. Sufficiently above  $\phi^*$ , the chain entanglement becomes significant and a transition to reptation-like behavior is predicted to occur. The critical concentration for entanglement is given by  $\phi_e \approx (M_e/M_w)^{0.75}$ , where  $M_e$  is the molecular weight between entanglement in melt.  $M_e \approx 2$  kg/mol so that PEG 5K is too short and there would not be enough number of entanglements per chain.<sup>22</sup> For 35K PEG,  $\phi_e$  is about 0.12. In the entangled regime another length scale, tube diameter  $a(\phi)$  needs to be considered,  $a(\phi) \approx a(1)\phi^{-0.76}$ , where  $a(1)$  is the tube diameter in the melt.<sup>18</sup> For PEG,  $a(1) \approx 4$  nm and  $a(\phi)$  ranges between 10 and 20 nm. Figure 1 shows schematically the relative size regimes covered in our experiments (also see Table S1).

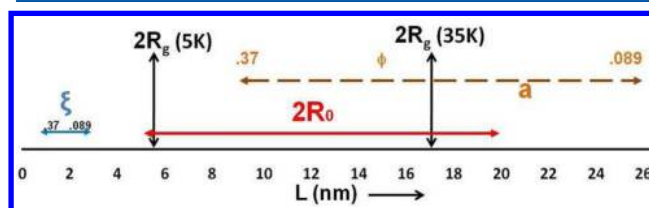


**Figure 1.** Schematic of different length scales covered in the experiments.

In Figure 2, we show some representative autocorrelation functions collected by FCS and plotted versus logarithmic time

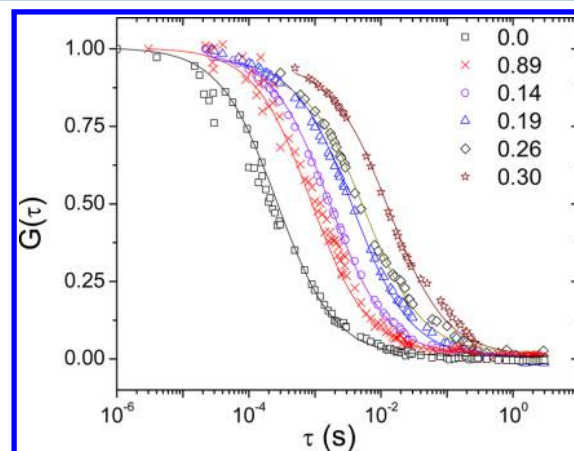


**Figure 2.** Normalized autocorrelation curves for Au NP ( $R_0 = 2.5$  nm) diffusion in PEG 35K solution at various polymer volume fractions. The curves are shifted to longer time scale as PEG concentration increases, indicating that diffusion coefficient decreases. The solid lines are fit of the curves.

lag. Each autocorrelation function was collected for about 15 min. The temperature was kept at room temperature (23 °C). To minimize the photothermal conversion from the excitation of the gold nanoparticles, the laser power was kept below 1 mW. Our estimation showed that the raise of the local temperature to be less than 0.1 °C, so the thermal effect did not



have any significant impact on the diffusive behavior of particles.<sup>13</sup> The FCS autocorrelation data of Au NPs in PEG was fitted using the equation mentioned earlier. The diffusion coefficients ( $D$ ) of Au NPs were calculated from the fit. Many different FCS trials were done for a given nanoparticle size for each polymer concentration on many different days with different samples. Trials were repeated for both molecular weights of PEG. Figure 3 shows the plot of  $D$  as a function of  $\phi$

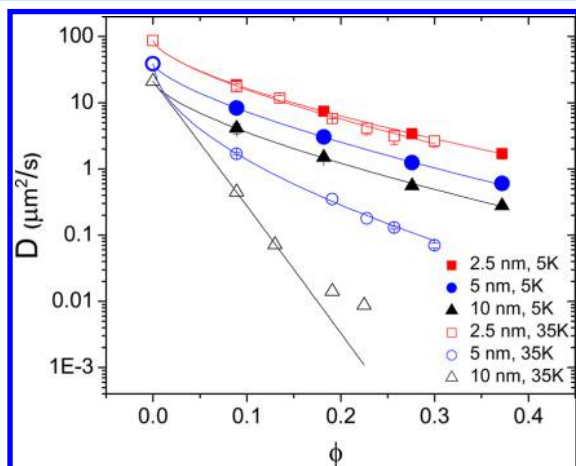


**Figure 3.** Diffusion coefficients as a function of polymer volume fraction. The solid lines show fits according to Phillies' equation. The caption indicates particle radii and the polymer molecular weight. The error bars are smaller than the size of the symbols. The fitting parameters are given in Table S3.

for three different nanoparticle sizes (see also Table S2). Each datum in the graph is the average, and the error bars are the standard deviation measured in more than 10 experiments.

First, we will compare the scaled diffusion coefficient ( $D/D_0$ ) data with Phillies' equation of stretched exponential function:  $D/D_0 \sim \exp(-\beta\phi^\nu)$  with  $\beta$  and  $\nu$  as adjustable parameters (Figure 3 and Table S3).<sup>6</sup> The fitting deviates from the data at higher concentrations. For PEG 35K at  $\phi = 0.26$  and  $R_0 = 10$  nm, the measured  $D$  is about an order of magnitude faster compared to the fit. At this concentration,  $\phi > \phi_c$  and  $2R_0 > a(\phi)$ . We speculate that effect on the particle motion due to network dynamics originating from chain reptation, which is not considered in Phillies' model becomes significant at concentrations above  $\phi_c$ . Consistent with some other reports,<sup>6,23</sup> we found that the exponent  $\nu$  lies between 0.56 and 1, but it does not have any clear dependence on the physical properties of the system, such as molecular weight of the polymer or the particle size. The parameter  $\beta$  is an increasing function of  $R_0$ . But it is to be noted here that the actual significance of these scaling exponents still lacks sound theoretical justification.

Next, we compare the measured diffusion coefficient with SE prediction using the bulk solution viscosity ( $\eta_m$ ). The macroscopic viscosity information on PEG–water solutions at various concentrations have been obtained from rheology data.<sup>14,27</sup> The ratio of measured  $D$  to calculated  $D_{SE}$  is plotted as a function of PEG concentration (Figure 4). For 5K PEG,  $R_0/R_g \geq 1$  for all particle sizes and we observed  $D/D_{SE} \approx 1$  and is independent of polymer concentration. For 35K PEG, the ratio shows positive deviation from unity and the deviation becomes stronger with increasing  $\phi$  and with the ratio  $R_0/R_g$  becoming smaller. For the lowest  $R_0/R_g$  as probed in our

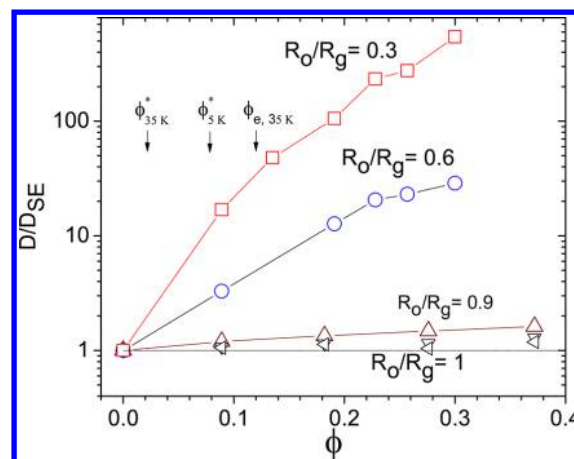


**Figure 4.** Ratio  $D/D_{SE}$  is plotted as a function of polymer volume fraction. SE behavior corresponds to the horizontal dashed line. As the ratio  $R_0/R_g$  becomes larger, the ratio approaches unity. Three particular concentrations are denoted.

experiments ( $\sim 0.3$ ), the NPs diffused 2–3 orders of magnitude faster compared to SE prediction. If  $\xi$  was the crossover length scale from nano- to macroviscosity, all the particles would have experienced the solution viscosity, and the SE relation would have correctly predicted the diffusion because  $R_0 \geq \xi$  for all cases investigated here. Thus, our results cannot be explained with some previous theories which concluded that  $\xi$  is the crossover length scale and  $D/D_{SE}$  should be independent of concentration when  $R_0 > \xi$ .<sup>9,17</sup> But it is in accord with results from computer simulations which characterizes  $R_g$  as the crossover length scale.<sup>29,30</sup> Similar conclusion was also drawn in experiments by Hoyst et al. using various dye and protein molecules but identifying  $R_0$  as the probe diameter instead of the radius. Our results do not necessarily contradict experiments by Lodge's group, where a return to SE behavior were obtained with increasing polymer concentration, as those were in the regime of  $R_0 > R_g$ .<sup>22</sup> For  $R_0 \leq R_g$ ,<sup>27</sup> the relative diffusion coefficients experienced by the particles was scaled as

$$\frac{D_0}{D} = \exp\left(\alpha\left(\frac{R_0}{\xi}\right)^\delta\right)$$

and for  $R_0 \geq R_g$  as

$$\frac{D_0}{D} = \exp\left(\alpha\left(\frac{R_g}{\xi}\right)^\delta\right)$$

with  $\alpha = 1.63 \pm 0.04$  and  $\delta = 0.89 \pm 0.02$ . Again our results are consistent with Holyst et al., besides the fact that  $R_0$  represents particle radius whereas they identified  $R_0$  as the particle diameter.<sup>14,27</sup> The scaled diffusion in these two equations makes SE relation applicable to particles of all sizes as is evident in Figure 5.

It is known that the presence of a depletion layer can reduce hydrodynamic resistance force compared to what is expected from the bulk viscosity as the particle moves through a medium of nonadsorbing polymer.<sup>8,26</sup> In the semidilute regime, the thickness of the depletion zone correlates with  $\xi$ ; hence, it is expected that its impact will be most significant for motion at the length scale of  $\xi$ , which is about 1–3 nm in our experiments. But FCS probes the diffusion set by the length scale of laser focus size ( $0.5 \mu\text{m}$ ). Assuming a depletion layer

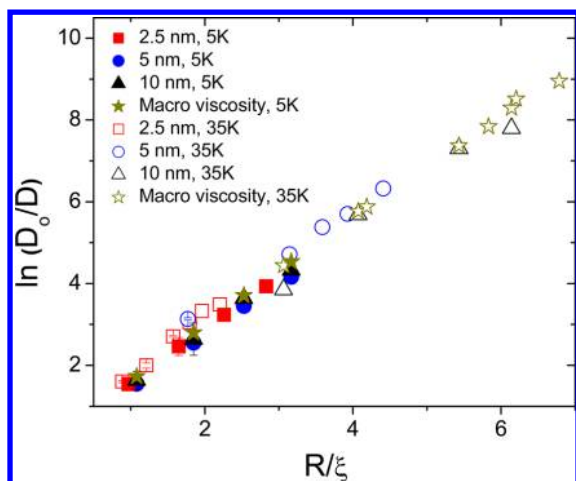


**Figure 5.** Normalized plot of  $D_0/D$  vs  $R/\xi$ , where  $R = R_g$  for  $R_0 \geq R_g$  and  $R = R_0$  for  $R_0 < R_g$ . All data points fall on a single curve.

thickness of  $l \sim 2$  nm and a particle ( $R_0 = 2.5$  nm) within the layer experience the neat solvent viscosity, the crossover time can be estimated as the  $\tau \approx l^2/6D_0 \sim 10$  ns, which is inaccessible in FCS experiments.<sup>27,34</sup> The nonuniform viscosity within the depletion layer could also induce slip and reduce the drag by a factor of 2/3.<sup>19,29,30</sup> But the deviation from SE prediction that we observed is much stronger.

To explain the observed deviation from SE-predicted diffusion for particle radii,  $R_0 < R_g$ , we consider the role played by the structural relaxation of the polymer matrix.<sup>35,36</sup> For 35K PEG, the polymer concentrations used in our experiments was about 5–10 times the overlap concentration and they fall in the semidilute entangled regime. The transport properties of the particle could be dominated by the reptation of the chains surrounding the particle.<sup>35</sup> Let us consider a particle with  $R_0 = 2.5$  nm radii in 35K PEG solution ( $R_0/R_g = 0.3$ ) at a polymer volume fraction of  $\phi \approx 0.2$ . We calculated the characteristic diffusion time of the particle,  $\tau_d \sim R_0^2/D$ , which is  $\sim 1$   $\mu$ s ( $D \approx 6$   $\mu$ m<sup>2</sup>/s). The characteristic time of polymer mesh relaxation by “constraint release”, also called the “tube renewal time”, can be estimated by using the relation  $\tau_r \sim 3\eta/G_N^0$ , where  $\eta$  is the viscosity and  $G_N^0$  is the plateau modulus of the polymer solution.<sup>12</sup> We have estimated that at  $\phi \approx 0.2$   $G_N^0 \sim 7.5 \times 10^4$  Pa. Taking the viscosity  $\eta \sim 1.6$  Pa·s,  $\tau_r \sim 0.1$  ms. Therefore,  $\tau_d \ll \tau_r$  and mesh is static in the time scale of particle motion, and the probe diffusion is not coupled to matrix relaxation.<sup>12</sup> The probe does not experience the macroscopic viscosity of the solution, and therefore  $D/D_{SE} \approx 100$ . For such situation, hydrodynamic models work relatively well to explain the particle diffusion. In the opposite limit, for a particle with radius,  $R_0 = 10$  nm in the same polymer solution ( $R_0/R_g \approx 1$ ),  $\tau_d \approx 7$  ms with  $D = 0.0141$   $\mu$ m<sup>2</sup>/s. Therefore,  $\tau_d \gg \tau_r$  and the motion of the particle is coupled with the matrix relaxation and  $D/D_{SE} \approx 1$  is obtained. The matrix relaxation must be taken into account to describe probe diffusion in these cases. We have not seen the return to SE behavior in the concentration regime that we explored. A future goal is to extend these measurements at a higher concentration to verify whether SE relation is eventually recovered.

Finally, we compare our data with the recent scaling theory of Cai et al.<sup>28</sup> The choice of the experimental system allowed us to compare two regimes: intermediate size particles ( $\xi < 2R_0 < a$ ) and large particles ( $2R_0 > a$ ). The theory predicts that the

intermediate size particles are affected by the segmental motion of the chains. At short times ( $t < \tau_\xi$ ) particle motion is diffusive, and the particle feels the solvent viscosity. In the intermediate time scale ( $\tau_\xi < t < \tau_x$ ), the motion is subdiffusive, and the particle feels a time-dependent viscosity. At longer times ( $t > \tau_x$ ), the motion is diffusive again, and the effective viscosity ( $\eta_{eff}$ ) felt by the particle is given by a polymer liquid consisting of chains comparable to the particle size,  $\eta_{eff} \sim \eta_s(R_0/\xi)^2$ . The time scales  $\tau_x$  and  $\tau_\xi$  correspond to the relaxation time of a polymer segment with size comparable to particle size  $2R_0$  and  $\xi$ , respectively. We have estimated that  $\tau_\xi < 1$  ns and  $\tau_x < 0.1$  ms, so our experiments measured the long-time diffusion. As  $\xi \approx \phi^{-0.76}$ ,  $D(\phi) \sim \phi^{-1.52}$  according to this theory for polymers in good solvent condition. Since both  $\xi(\phi)$  and  $a(\phi)$  are concentration dependent, it is important to consider two crossover concentrations. This first one is  $\phi^\xi$  at which  $\xi \approx 2R_0$ . For an athermal solvent it can be estimated by the expression,  $\phi^\xi \approx \phi^*(R_g/2R_0)^{1.32}$ . The other important concentration is  $\phi^a$  at which  $a(\phi) \approx 2R_0$ . It can be estimated by making use of the expression  $\phi^a \approx (2R_0/a(1))^{-1.32}$ . Between  $\phi^\xi$  and  $\phi^a$ , the particle size corresponds to the intermediate size regime. Accordingly, the 2.5 nm radius Au NPs can be classified as intermediate sized between volume fraction 0.04 and 0.74 (details available in Supporting Information Table S1). The volume fraction in our experiments was varied from 0.09 to 0.37. It was observed that these particles follow a power law dependence of the measured diffusion on the volume fraction:  $D(\phi) \propto \phi^{-1.45 \pm 0.09}$  (Figure 6). Our results are in good

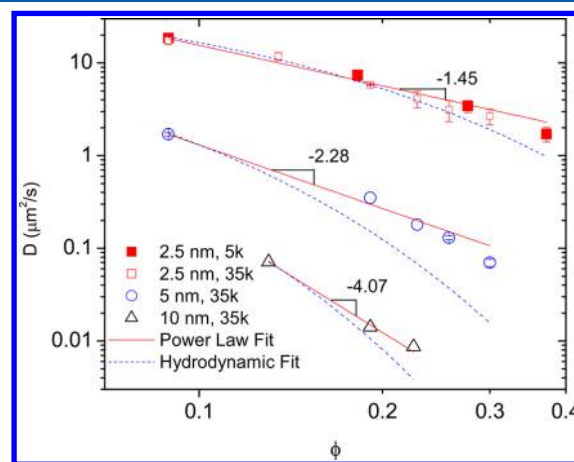


**Figure 6.** Power-law dependence of diffusion coefficients on volume fraction. The data for particles with radii 5 and 10 nm in 5K PEG were not included as in these situations,  $R_0 > R_g$ . The figure also showed the hydrodynamic fit, which gives a stretched exponential dependence on polymer volume fraction with exponent  $\nu = 0.76$ . Table S3 lists all the fitting parameters used in this figure.

agreement with the scaling model according to which the particle diffusion coefficient decreases with solution volume fraction as power  $-1.52$  for athermal solvent.<sup>28</sup>  $D$  is expected to be independent of  $M_w$  in this regime as long as the tube diameter or polymer size is larger than  $R_0$ . For particle with  $R_0 = 2.5$  nm in 5K PEG solution,  $R_0 \approx R_g$ , so the above condition is approximately satisfied, but we still have observed near independence of polymer  $M_w$  on particle diffusion. In the intermediate size regime, the effective viscosity is proportional to the particle surface area; hence,  $D$  is proportional to  $R_0^{-3}$ . To test this prediction, we needed particles of different sizes at a

fixed concentration of a particular molecular weight polymer. At volume fraction of  $\phi = 0.089$  the 5 nm radii particles fall well in intermediate sized regime. Analyzing the intermediate sized 2.5 and 5 nm particles at this concentration for 35K PEG gives  $D(R_0) \sim R_0^{-3.36}$ . Since 5 nm radii particles get into the transition of intermediate to large sized particles with the increase in volume fraction, we could not test this scaling relation for other concentrations. These particles ( $R_0 = 5$  nm) showed a slightly different behavior than that predicted in the literature.<sup>28</sup> It can be attributed to the fact that in the concentration range studied these particles are at the transition of intermediate and large sized particles. The diffusion still followed a power law dependence on the volume fraction though with a slightly different power:  $D(\phi) \propto \phi^{-2.28 \pm 0.1}$  (Figure 6).

The volume fractions equal or above  $\phi^a$  correspond to large particle regime,  $2R_0 > a(\phi)$ . The diffusion for large particles can occur through the reptation of the surrounding polymer chains and from the temporal fluctuation of the local matrix. The motion due to chain reptation is diffusive at long times and is determined by the bulk viscosity ( $\eta_m$ ) of entangled liquid. SK PEG solutions are not entangled at any concentrations; for 35K PEG solution, this regime is obtained above a threshold concentration,  $\phi^a \approx 0.12$  for  $R_0 = 10$  nm. Our data showed  $D$  decreases strongly with increasing concentration above  $\phi^a$ . The decrease is well-fitted by the power law  $D(\phi) \sim \phi^{-4.07 \pm 0.19}$  compared to the theoretical prediction of the exponent  $-3.93$  in athermal solvent. The diffusion coefficient is expected to be inversely proportional to the nanoparticle radius as in SE relation. Since we only had 10 nm particles in large particle regime, we did not have sufficient data to test this relation. But as our measured diffusion values for the particle show a return to SE behavior, it implies that for even larger particles, this relation would have followed. In Figure 6 we have also shown the prediction from hydrodynamic theory<sup>7</sup> which gives the functional form  $D/D_0 \sim \exp(-\kappa R_0/\xi)$ , treating  $\kappa$  as the only adjustable parameter. In this situation, the power law fits better, particularly in the large particle regime. This indicated that polymer motion plays an important role, and treating the matrix as fixed in time is inadequate to describe the nanoparticle dynamics in macromolecular solution.

## CONCLUSION

We measured the diffusion of gold nanoparticles of radii 2.5–10 nm in semidilute poly(ethylene glycol) (PEG)–water solution by using fluctuation correlation spectroscopy. For particles with radii  $R_0 > R_g$ , measured diffusion coefficients were similar to that expected by SE relation using the macroscopic viscosity for the polymer solution, whereas for particles with radii  $R_0 \leq R_g$ , the diffusion is faster than that estimated from SE relation. The ratio  $D/D_{SE}$  increases with polymer concentration and as  $R_0/R_g$  becomes smaller. The results were rationalized by comparing the characteristic time of probe diffusion with the time scale of constraint release dynamics for entangled polymer. We compared our results with currently available theories. A reasonably good agreement was found with the recent scaling theory, which takes into account the role of polymer dynamics on particle diffusion. Our results will be important for understanding intracellular transport of globular molecules<sup>3</sup> and for the development of novel therapeutic treatments, which rely upon delivery of nanoparticles through complex spatial structures, such as mucin network.<sup>2</sup>

## ASSOCIATED CONTENT

### Supporting Information

One figure and three tables, including the TEM image of gold nanoparticles with histogram analysis, tables for important length scales and other parameters, data for diffusion coefficients as a function of polymer volume fraction, and fitting parameters used in analyzing the figures. This material is available free of charge via the Internet at <http://pubs.acs.org>.

## AUTHOR INFORMATION

### Corresponding Author

\*E-mail [ashis@wayne.edu](mailto:ashis@wayne.edu); Tel 313-577-2775; Fax 313-577-3932.

### Notes

The authors declare no competing financial interest.

## ACKNOWLEDGMENTS

Acknowledgements are made to the National Science Foundation through Grant DMR-0605900 and Wayne State University Bridge Fund program for support of this research. We thank Prof. Michael Rubinstein and Liheng Cai for valuable discussions.

## REFERENCES

- (1) Russel, W. B.; Saville, D. A.; Schowalter, W. R. *Colloidal Dispersions*; Cambridge University Press: Cambridge, UK, 1989.
- (2) Cu, Y.; Saltzman, W. M. *Nat. Mater.* **2009**, *8*, 11.
- (3) Zhou, H.-X.; Rivas, G.; Minton, A. P. *Annu. Rev. Biophys.* **2008**, *37*, 375.
- (4) Solomon, M. J.; Lu, Q. *Curr. Opin. Colloid Interface Sci.* **2001**, *6*, 430.
- (5) Liu, J.; Zhang, L.; Cao, D.; Wang, W. *Phys. Chem. Chem. Phys.* **2009**, *11*, 11365.
- (6) Phillies, G. D. J. *Macromolecules* **1987**, *20*, 558.
- (7) Cukier, R. I. *Macromolecules* **1984**, *17*, 252.
- (8) Tuinier, R.; Fan, T. H. *Soft Matter* **2008**, *4*, 254.
- (9) Langevin, D.; Rondelez, F. *Polymer* **1978**, *19*, 875.
- (10) Ganesan, V.; Pryamitsyn, V.; Surve, M.; Narayanan, B. J. *Chem. Phys.* **2006**, *124*, 221102.
- (11) Masaro, L.; Zhu, X. X. *Prog. Polym. Sci.* **1999**, *24*, 731.
- (12) Cheng, Y.; Prud'homme, R. K.; Thomas, J. L. *Macromolecules* **2002**, *35*, 8111.
- (13) Omari, R.; Aneese, A.; Grabowski, C.; Mukhopadhyay, A. J. *Phys. Chem. B* **2009**, *113*, 8448.
- (14) Holyst, R.; Bielejewska, A.; Szymanski, J.; Wilk, A.; Patkowski, A.; Gapinski, J.; Zywockinski, A.; Kalwarczyk, T.; Kalwarczyk, E.; Tabaka, M.; Ziebach, N.; Wieczorek, S. A. *Phys. Chem. Chem. Phys.* **2009**, *11*, 9025.
- (15) Koenderink, G. H.; Sacanna, S.; Aarts, D. G. A. L.; Philipse, A. P. *Phys. Rev. E* **2004**, *69*, 021804.
- (16) Lin, T. H.; Phillies, G. D. J. *J. Phys. Chem.* **1982**, *86*, 4073.
- (17) de Gennes, P.-G. *Scaling Concepts in Polymer Physics*; Cornell University Press: Ithaca, NY, 1979.
- (18) Rubinstein, M.; Colby, R. H. *Polymer Physics*; Oxford University Press: New York, 2003.
- (19) Brochard Wyart, F.; de Gennes, P. G. *Eur. Phys. J. E* **2000**, *1*, 93.
- (20) Tong, P.; Ye, X.; Ackerson, B. J.; Fetters, L. J. *Phys. Rev. Lett.* **1997**, *79*, 2363.
- (21) Ye, X.; Tong, P.; Fetters, L. J. *Macromolecules* **1998**, *31*, 5785.
- (22) Won, J.; Onyenemezu, C.; Miller, W. G.; Lodge, T. P. *Macromolecules* **1994**, *27*, 7389.
- (23) Michelman-Ribeiro, A.; Horkay, F.; Nossal, R.; Boukari, H. *Biomacromolecules* **2007**, *8*, 1595.
- (24) Phillies, G. D. J.; Clomenil, D. *Macromolecules* **1993**, *26*, 167.
- (25) Ullmann, G. S.; Ullmann, K.; Lindner, R. M.; Phillies, G. D. J. *J. Phys. Chem.* **1985**, *89*, 692.

- (26) Fan, T. H.; Dhont, J. K. G.; Tuinier, R. *Phys. Rev. E* **2007**, *75*, 011803.
- (27) Ziebac, N.; Wieczorek, S. A.; Kalwarczyk, T.; Fiakowski, M.; Holyst, R. *Soft Matter* **2011**, *7*, 7181.
- (28) Cai, L.-H.; Panyukov, S.; Rubinstein, M. *Macromolecules* **2011**, *44*, 7853.
- (29) Liu, J.; Cao, D.; Zhang, L. *J. Phys. Chem. C* **2008**, *112*, 6653.
- (30) Egorov, S. A. *J. Chem. Phys.* **2011**, *134*, 084903.
- (31) Onyenemezu, C. N.; Gold, D.; Roman, M.; Miller, W. G. *Macromolecules* **1993**, *26*, 3833.
- (32) Grabowski, C.; Adhikary, B.; Mukhopadhyay, A. *Appl. Phys. Lett.* **2009**, *94*, 021903.
- (33) Devanand, K.; Selser, J. C. *Macromolecules* **1991**, *24*, 5943.
- (34) Ochab-Marcinek, A.; Holyst, R. *Soft Matter* **2011**, *7*, 7366.
- (35) Graessley, W. W. *Adv. Polym. Sci.* **1982**, *47*, 67.
- (36) Pryamitsyn, V.; Ganesan, V. *Phys. Rev. Lett.* **2008**, *100*, 128302.